Original Article

Personalized dosimetry for a deeper understanding of metastatic response to high activity ^{131}I-mIBG therapy in high risk relapsed refractory neuroblastoma

Bartolomeo Cassano[1]^, Milena Pizzoferro[2], Silvio Valeri[1], Claudia Polito[1], Salvatore Donatiello[1], Claudio Altini[2], Maria Felicia Villani[2], Annalisa Serra[3], Aurora Castellano[2,3], Maria Carmen Garganese[2], Vittorio Cannatà[1]

[1]Medical Physics Unit, IRCCS Bambino Gesù Children's Hospital, Rome, Italy; [2]Nuclear Medicine Unit/Imaging Department, IRCCS Bambino Gesù Children's Hospital, Rome, Italy; [3]Department of Pediatric Hematology and Oncology, IRCCS Ospedale Pediatrico Bambino Gesu, Rome, Italy

Contributions: (I) Conception and design: B Cassano, M Pizzoferro, S Valeri; (II) Administrative support: C Polito, S Donatiello, C Altini, MF Villani; (III) Provision of study materials or patients: A Serra, A Castellano, MC Garganese, M Pizzoferro, C Altini, MF Villani; (IV) Collection and assembly of data: B Cassano, M Pizzoferro, S Valeri, C Polito, S Donatiello, V Cannatà; (V) Data analysis and interpretation: B Cassano, M Pizzoferro, S Valeri, MC Garganese, V Cannatà; (VI) Manuscript writing: All authors; (VII) Final approval of manuscript: All authors.

Correspondence to: Bartolomeo Cassano. Via Portuense, 391 Rome, Italy. Email: bartolomeo.cassano@gmail.com.

Background: Dosimetry in molecular radiotherapy for personalized treatment is assuming a central role in clinical management of aggressive/relapsed tumors. Relapsed/refractory metastatic high-risk neuroblastoma (rrmHR-NBL) has a poor prognosis and high-activity ^{131}I-mIBG therapy could represent a promising strategy. The primary aim of this case series study was to report the absorbed doses to whole-body (D_{WB}), red marrow (D_{RM}) and lesions (D_{Lesion}). A secondary aim was to correlate D_{Lesion} values to clinical outcome.

Methods: Fourteen patients affected by rrmHR-NBL were treated with high-activity ^{131}I-mIBG therapy (two administrations separated by 15 days). The first administration was weight-based whereas the second one was dosimetry-based (achieving D_{WB} equals to 4 Gy). In all patients D_{WB} and D_{RM} was assessed; 9/14 patients were selected for D_{Lesion} evaluation using planar dosimetric approach (13 lesions evaluated). Treatment response was classified as progressive and stable disease (PD and SD), partial and complete response (PR and CR) according to the International Neuroblastoma Response Criteria. Patients were divided into two groups: Responder (CR, PR, SD) and Non-Responder (PD), correlating treatment response to D_{Lesion} value.

Results: The cumulative D_{WB}, D_{RM} and D_{Lesion} ranged from (1.5; 4.5), (1.0; 2.6) and (44.2; 585.8) Gy. A linear correlation between D_{WB} and D_{RM} and a power law correlation between the absorbed dose to WB normalized for administered activity and the mass of the patient were observed. After treatment 3, 2, 4 and 5 patients showed CR, PR, SD and PD respectively, showing a correlation between D_{Lesion} and the two response group.

Conclusions: Our experience demonstrated feasibility of high activity therapy of ^{131}I-mIBG in rrmHR-NBL children as two administration intensive strategy. Dosimetric approach allowed a tailored high dose treatment maximizing the benefits of radionuclide therapy for pediatric patients while maintaining a safety profile. The assesment of D_{Lesion} contributed to have a deeper understaning of metabolic treatment effects.

Keywords: Dosimetry; ^{131}I-mIBG high activity therapy; dose-response correlation; high risk neuroblastoma

^ ORCID: 0000-0001-5747-8230.

Submitted May 21, 2021. Accepted for publication Sep 06, 2021.
doi: 10.21037/qims-21-548
View this article at: https://dx.doi.org/10.21037/qims-21-548

Introduction

Treatment of relapsed/refractory metastatic high-risk neuroblastoma (rrmHR-NBL) after multimodality therapy remains a clinical challenge; despite recent advances in our understanding of neuroblastoma biology and new treatment strategies, the outcome for children affected by rrmHR-NBL remains poor with a 5 years overall survival around 20% (1,2).

Approximately 90% of neuroblastoma cases accumulate the noradrenalin analogue metaiodobenzylguanidine (mIBG) by a specific uptake mechanism and ^{131}I-mIBG can be used for targeted radiotherapy delivering a focal dose of radiation to the tumor sites. A 30–40% response rate has been observed in refractory and relapsed neuroblastoma (3,4) and the application of target radiotherapy in new sequential treatments with various drugs is under clinical assessment. Among sequential treatment strategies for rrmHR-NBL, high activity mIBG can be combined with chemotherapy followed by autologous stem cell transplantation (ASCT) (5,6). Thus, children with rrmHR-NBL continue to need combinations of different therapeutic modalities to prolong survival and minimize the toxicities of additional therapies.

In 2005, Gaze *et al.* (7) demonstrated the feasibility of high activity mIBG therapy based on dosimetric approach combined with chemotherapy. The rationale of this study protocol is based on two high activity ^{131}I-mIBG administrations guided by a dosimetric assessment to achieve a whole-body (WB) absorbed dose of 4 Gy.

This paper will focus on reporting our experience in dosimetric assessment in children affected by rrmHR-NBL treated with high activity mIBG therapy, underlying the correlation between WB and red marrow (RM) absorbed dose and demonstrating the usefulness of lesions dosimetry.

We present the following article in accordance with the STROBE reporting checklist (available at https://dx.doi.org/10.21037/qims-21-548).

Methods

Patients

The study was conducted in accordance with the Declaration of Helsinki (as revised in 2013). The study was approved by ethics committee of IRCCS Bambino Gesù Children's Hospital and informed consent was taken from all individual participants. In the present case series study, 14 patients (7 boys and 7 girls with ages ranging from 3 to 17 years) with rrmHR-NBL (previously treated according standard procedure for HR-NBL) have been enrolled and submitted to high activity ^{131}I-mIBG administrations at "Bambino Gesù" Children Hospital, recruited over a period of 3 years since 2017. The age at the time of the initial diagnosis ranged from 1 to 17 years (median 4 years). The treatment protocol was based on a scheme consisting of two ^{131}I-mIBG administrations 2 weeks apart followed by a single dose of Melphalan (110 mg/m^2) 96 hours after the second ^{131}I-mIBG administration and autologous stem cell transplantation 24 hours after the end of chemotherapy.

First ^{131}I-mIBG administration was weight-based (approximately 444 MBq/kg, excepted for 5 patients over 50 kg of weight who received no more than 17 GBq due to legal limit), whereas the second administration was dosimetry based in order to achieve an absorbed dose to WB (D_{WB}) equals to 4 Gy as suggested by Gaze *et al.* (7). Patients over 50 kg of weight received a second administration of 17 GBq achieving a total absorbed dose to WB as high as possible.

Thyroid protection block was performed in all patients by administration of Lugol solution and triiodothyronine since 72 h before the first mIBG treatment to 15 days after the second one. mIBG avid disease was proven by ^{123}I-mIBG scan to evaluate basal status disease and clinical response after treatment. ^{123}I-mIBG scans were assessed according to the SIOPEN-mIBG scoring system (8) and the clinical response after ^{131}I-mIBG therapy was classified as progressve and stable disease (PD and SD) or partial and complete response (PR and CR) according to the International Neuroblastoma Response Criteria (INRC) Definition of Response (9) within a range from 1 to 3 months.

All patients who had a therapeutic effect (such as complete response, partial response or stable disease) were included in the "Responder group" while patients in progression disease were assigned to "Non-Responder group".

WB/RM dosimetry

Each patient was submitted to 6 or 7 dose rate measurements (R) to assess whole-body cumulated activity ($\tilde{A}_{WB}$). Measurements were performed in anterior and posterior views, using a Geiger counter placed 2 m from the patient for a duration of 3 min. The first measurements [$R_A(0)$ and $R_P(0)$] were performed immediately after ^{131}I-mIBG administration, in order to avoid bladder emptying and measure the dose rate of the total administered activity; the next measurements were performed after bladder emptying with the following time sampling 1, 6, 24, 48, 54, 166 h after tracer administration; background activity was registered before each time point. The activity at time t was calculated using the following formula:

$$A_{WB}(t) = A_{Adm} \cdot \sqrt{\frac{R_A(t) \cdot R_P(t)}{R_A(0) \cdot R_P(0)}} \quad [1]$$

where A_{Adm} is the activity administer and R_A and R_P are the dose rates, in anterior and posterior views, considering background correction.

With an analogous time sampling, six blood samples have been collected (with a volume of about 3 mL) using a central line catheter previously placed for clinical purpose. Blood sample activities were assessed after 2 weeks to reduce dead-time effects, thanks to a gamma counter. Blood activity concentration {[$A_{Blood}(t)$]} was calculated as follows:

$$\left[A_{Blood}(t)\right] = CPS \cdot \frac{C_{GC}}{m_{Blood}} \quad [2]$$

where CPS (Counts Per Second) is the output signal of the gamma counter after a measurement of 10 min, C_{GC} is the gamma counter calibration factor which transforms CPS into activity taking into account the geometric deviations due to different masses for each blood sample (m_{Blood}).

The calculation of $\tilde{A}_{WB}$ and [$\tilde{A}_{Blood}$] has been performed using by NukFit software (10). With this software it was possible to choose the best fit model, competing a mono and bi exponential fit using the AICc method (11), and to calculate the area under the curve.

According to EANM guidelines D_{WB} has been calculated using the following formula (12):

$$D_{WB} = \tilde{A}_{WB} \cdot S_{WB \leftarrow WB} \quad [3]$$

Using an S-factors given by the following formula (13,14):

$$S_{WB \leftarrow WB} = 1.34 \cdot 10^{-4} \cdot m_p^{-0.921} \left[\frac{Gy}{MBq \cdot h}\right] \quad [4]$$

where m_p is the patient's weight.

Whereas, the D_{RM} is the sum of two contributions: (I) direct irradiation due to blood activity (self blood contribution) and (II) indirect irradiation due to rest of body activity. It has been calculated using the formula reported in (15,16):

$$D_{RM} = RMBLR \cdot \left[\tilde{A}_{Blood}\right] \cdot m_{RM} \cdot S_{RM \leftarrow RM} + \\ + \left(\tilde{A}_{WB} - RMBLR \cdot \left[\tilde{A}_{Blood}\right] \cdot m_{RM} \cdot \frac{m_p}{m_{WB}}\right) \cdot \frac{m_{WB}}{m_p} \cdot S_{RM \leftarrow RoB} \quad [5]$$

where m_{WB} and m_{RM} are the body mass and RM, the mass of a standard phantom, respectively; RMBLR is the radioactive concentration ratio between marrow and blood, set equal to 1 and S-Factors are taken by Olinda (17).

Lesion dosimetry

The conjugate views method described in Pamphlet MIRD 16 (18) was used to calculate the absorbed dose to patient's lesions using static planar scintigraphic images. Evaluation of 13 lesions in 9 patients detailed the following features: (I) lesions were qualitatively detectable by tumor delineation both on CT images and on scintigrafic images after the administration of ^{131}I-mIBG; (II) lesions were to be non-retrohepatic.

Each of these patients underwent a specific acquisition protocol consisting of a CT scan, a trasmissive acquisition (before the first administration of ^{131}I-mIBG) and a series of static images after the first and the second therapeutic administration.

A CT scan of the body's segment including the lesion's site was performed within a range of 1–3 months before ^{131}I-mIBG therapy. By contouring the tumor's edges on this scan, the volume and the mass of the lesion were calculated considering a density equal to 1 in case of soft tissue.

In order to estimate the patient's body thickness along lesion's view (T), 1 h before ^{131}I-mIBG administration, two transmissive images (one without the patient - blank - and the other with the patient) were acquired using a source of ^{99m}Tc of about 37 MBq and LEHR collimators.

A series of static scintigraphic acquisitions were also collected after the first and the second administration. The acquisition parameters are reported in *Table 1*.

The scintigraphic images were subsequently corrected for scatter, using the Ogawa method (19), and for dead time placing a known source (of about 11.1 MBq) in the field of view, avoiding the overlap on patient's body and normalising the total counts acquired within the image to those obtained from the source without the patient present (20). The lesion

Table 1 Acquisition parameters for scintigraphic images

Parameters	Data
Time	5 min
Time sampling	2, 6, 24, 36, 144–166 h
Matrix	128×128
Collimator	HE
Primary Energy Window	363.8 keV ±7.5%
Lower Energy Window	309.2 keV ±7.5%
Upper Energy Window	418.3 keV ±7.5%

was delineated on the first image of the series and, in order to improve the placement of lesion's region of interest (ROI), all (scintigraphic and trasmissive) planar images were co-registered referring to the first scintigraphic image acquired.

Following the Pamphlet MIRD 16 lesion's activity at time t was calculated according to the formula showed in (18):

$$A_{Lesion}(t) = \sqrt{\frac{I_{Ant}(t) \cdot I_{Post}(t)}{e^{-\mu(I-131)\cdot T}}} \cdot \frac{f_j}{C} \quad [6]$$

where I_{Ant} and I_{Post} represent counts inside lesion's ROI in anterior and posterior views respectively, corrected for background; f_j is the self attenuation correction; C and $\mu(I\text{-}131)$ are the sensitivity of the gamma camera and the attenuation coefficient for ^{131}I obtained using an abosolute quantification described in (15,21) and are equal to 12.83 cps/MBq and 0.106 cm^{-1}, respectively.

Finally the absorbed dose to lesion (D_{Lesion}) was calculated using the formula:

$$D_{Lesion} = \tilde{A}_{Lesion} \cdot S_{Lesion \leftarrow Lesion} \quad [7]$$

where $\tilde{A}_{Lesion}$ is the cumulated activity, calculated by Nukfit in the same way as described for the WB and $S_{Lesion \leftarrow Lesion}$ using the values obtained by the interpolation of S-value of the spheres taken from the Olinda software.

A possible therapeutic dose-response correlation was also assessed comparing the cumulative doses to lesions in "Responder" and "Non-Responder" patients group by statistical analysis described in the next section.

Statistical analysis

Descriptive statistics tools (as mean, standard deviation and median) were used for describing the dosimetric results.

Correlation between D_{WB} and D_{RM} were determined by linear regression analysis.

Table 2 Patient's characteristics and the relative clinical response to ^{131}I-mIBG therapy

Patient ID	Gender	Age at treatment, years	Weight, kg	Disease status after two ^{131}I MIBG therapies
Pat - 1	M	8	27	PD
Pat - 2	M	17	87	CR
Pat - 3	F	9	21	SD
Pat - 4	F	4	14	CR
Pat - 5	F	4	18	CR
Pat - 6	M	17	54	PR
Pat - 7	M	12	68	PR
Pat - 8	F	6	21	PD
Pat - 9	F	16	57	SD
Pat - 10	M	6	20	SD
Pat - 11	F	3	12	PD
Pat - 12	M	6	20	SD
Pat - 13	M	13	71	PD
Pat - 14	F	3	12	PD

Power-Law fit were used to estimate the correlation between D_{WB} and mass of the patient.

Correlation between clinical response (categorical factor) and D_{Lesion} (continuous variable) was assessed by the Mann-Whitney test.

Results

Clinical results

Main patient's characteristics and the relative clinical response to ^{131}I-mIBG therapy are summarized in *Table 2*. No patients showed acute toxicity (hypertensive crisis or other heavy side effects); nausea and vomiting were well controlled by antiemetic drugs. Medullary aplasia was obtained in all patients as required by treatment protocol scheme. All patients had demonstrated progressive disease on the ^{123}I-mIBG pre-therapy scan with a SIOPEN score greater than 3. After ^{131}I-mIBG therapy 5/14 patients (35.7%) showed progressive disease while 4/14 (28.6%) patients showed stable disease. Two patients (14.3%) showed partial response and 3 (21.4%) patients showed a complete response.

The "Responder group" rate, considering all those

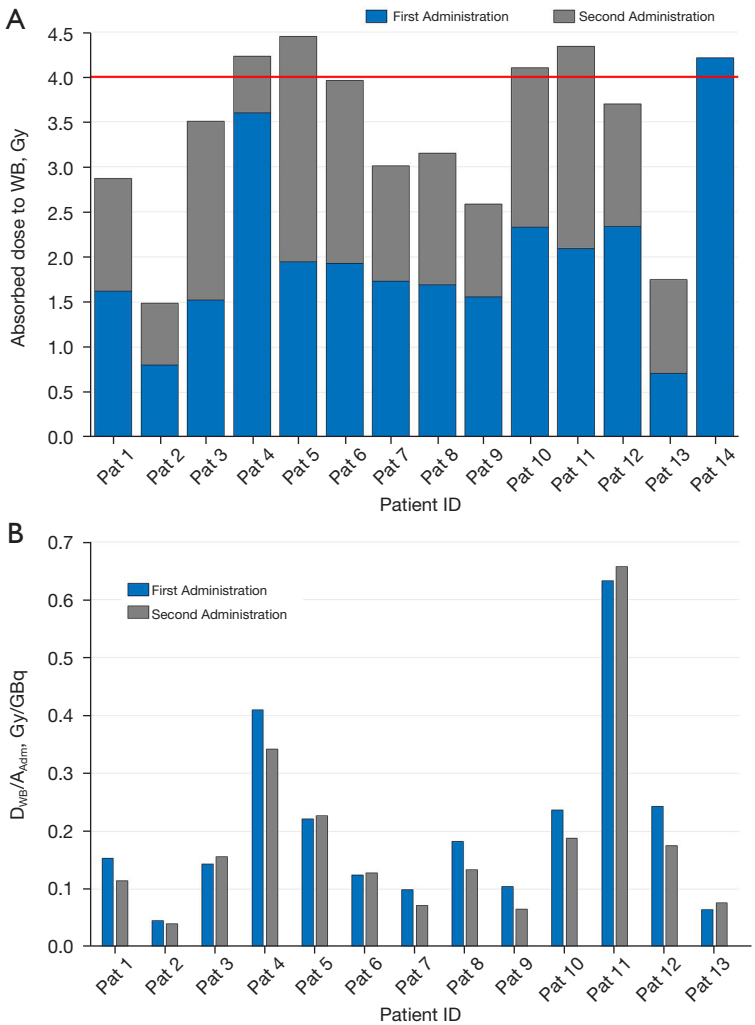

Figure 1 Dosimetric results related to WB. (A) Total absorbed dose to WB distribution referring to the limit threshold of 4 Gy (red line), after two treatments (excluding patient number 14 who didn't receive the second treatment). (B) Comparison between D_{WB}/A_{Adm} values assessed at first (blue) and at second (gray) administration.

patients who had a therapeutic effect (such as complete response, partial response or stable disease), was 64.3%. "Non Responder group" rate (progression disease) was 35.7%.

Absorbed dose to WB/RM results

The biokinetic chosen varied for each patient resulting 6/14 and 5/14 mono exponential fit for WB and RM respectively, remaing the same fit-model from the first to the second administration.

On the base of the D_{WB} assessment at the first administration, 13 patients received a full treatment while only one patient received a single dose administration due to the delivery of a D_{WB} value of 4.2 Gy. The injected activities at the second administration to obtain a complete treatment were in the range of 1.8 to 17.9 GBq (median 11.0 GBq) while the total activity administered was between 2.2 and 35.4 GBq (median 20.8 GBq).

The media (range) of D_{WB} values for single administration was 1.7 (0.6–4.2) Gy. The absorbed dose obtained summing the results of the two administrations was 3.6 (1.5–4.5) Gy.

In *Figure 1A*, the cumulated absorbed doses to WB for the 14 treated patients are reported.

Considering the 13 patients who completed two administrations, in *Figure 1B*, D_{WB}/A_{Adm} values of 13 patients are reported obtaining values ranging to 0.15

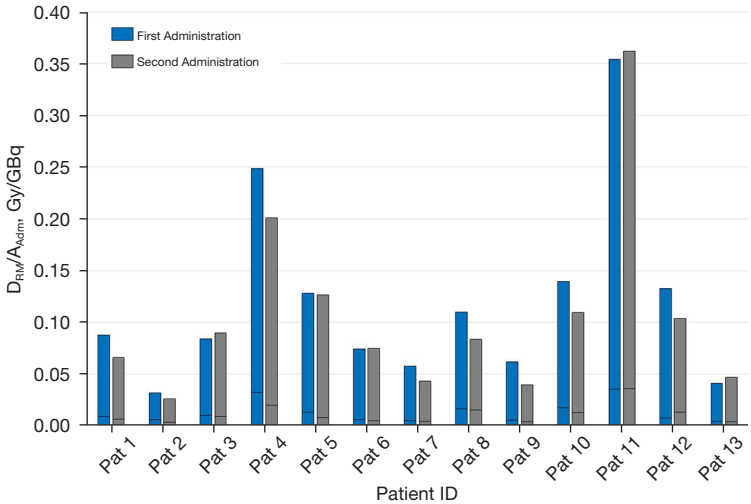

Figure 2 Comparison between D_{RM}/A_{Adm} values assessed at first (blue) and at second (gray) administration. Stacked bars for each administration divide self-blood (lower area) from the rest of body contribution.

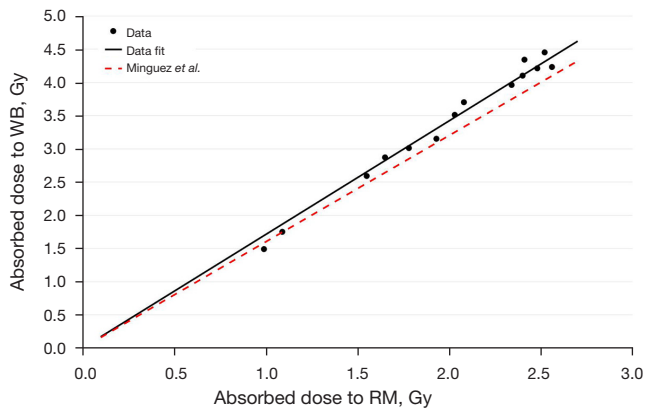

Figure 3 Linear fit of D_{RM} and D_{WB} data and comparison with the result obtained by Minguez *et al.* (22).

(0.04–1.91) Gy/GBq. The percentage difference of D_{WB}/A_{Adm} (normalized dose to administered activity) between the first and second administration was between −37.0% and 18.5% with a median of −16.5%. Eight out of 13 patients (61.5%) showed a reduction in the absorbed dose per unit of administered activity between the first and second treatment, while 4 out of 13 patients (30.8%) showed an increase in D_{WB}/A_{Adm} of less than 10%.

A tight range of the blood samples mass was measured 2.5–3.1 g minimizing geometric effects. D_{RM} values for each administration was 1.0 (0.4–2.5) Gy. The absorbed dose obtained summing the results of the two administrations was 2.1 (1.0–2.6) Gy. In *Figure 2*, D_{RM}/A_{Adm} values of 13 patients who received two administrations are reported showing a blood self contribution ranging from 5.7% to 19.2% with a median value of 10.0% respect to the D_{RM} value. The percentage difference of D_{RM}/A_{Adm} between the first and the second administration were between −57.0% and 13.1% with a median value of −23.8%. In particular, 9/13 patients (69.2%) showed a reduction of D_{RM}/A_{Adm}, while 3/13 patients (23.1%) showed an increase of D_{RM}/A_{Adm} inferior to 10%.

In *Figure 3*, the trend of the absorbed dose to RM respect to the dose to WB are reported. The graph shows a strong linear correlation between the two parameters with an angular coefficient a R^2 equal to 1.7, 0.9922 respectively ($P<0.01$).

Figure 4 showed the correlation between D_{WB}/A_{Adm} versus the mass of the patient obtaining the following result:

$$\frac{D_{WB}}{A_{Adm}} = 3.48 \cdot m^{-0.921} \quad [8]$$

Absorbed dose to lesion results

The number of detected lesion following the mentioned inclusion criteria was 13 in 9 patients and their anatomical features and dosimetric results were reported in *Table 3*.

The distribution of lesions in different anatomical districts was heterogeneous with a volume range of 0.4–246.4 cm^3 from the cervical district to the low abdomen.

The absorbed doses delivered from single administration were between 6.3 and 300.9 Gy with a median 81.8 Gy while the total absorbed dose of the two administrations ranged from 44.2 and 585.8 Gy, with a median of 164.3 Gy. D_{Lesion}/A_{Adm} was within the range of 0.9 to 26.1 Gy/GBq with a median of 8.6 Gy/GBq. The percentage difference in D_{Lesion}/A_{Adm} between the second and the first administration was between −76.8% and 21.0% with a median of −44.7%. In *Figure 5*, D_{Lesion}/A_{Adm} values of 13 lesions for each administration are reported. 10/13 (76.9%) lesions showed a reduction of the uptake at the second administration compared to the first (percentage differences ranged from −76.9% to −22.6%); 2/13 (15.4%) lesions had a similar values and only in one case there is an increase of the uptake equals to 21.0%.

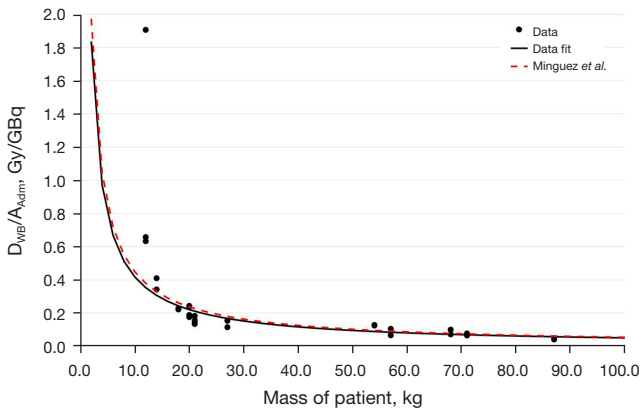

Figure 4 Power law fit of D_{WB}/A_{Adm} versus the mass of the patients and comparison with the curve obtained by Minguez *et al.* (22).

We also assessed a possible therapeutic dose-response correlation showed in *Figure 6*.

The median of the Non-Responder group was 82.0 Gy, while that one of the Responder group was 258.2 Gy. The minimum value present in the Responder group was 44.2 Gy. The Mann-Whitley U test showed that the median absorbed doses were significantly different in the two groups (P=0.0196).

Discussion

Our experience demonstrated feasibility of high activity therapy of ^{131}I-mIBG in rrmHR-NBL children as two administration intensive strategy. As shown by Genolla *et al.* (23), the use of personalized dosimetry in combination with the clinical data confirms that protocol theorized by Gaze *et al.* (7) is a safe treatment strategy.

Dosimetric approaches allow a tailored high dose treatment maximizing the benefits of radionuclide therapy for pediatric patients.

The graph in *Figure 1A* shows that the summed dose

Table 3 Summary table of the dosimetric parameters evaluated on the lesions

Lesion ID	Contouring lesion site	Volume (cm^3)	First administration		Second administration	
			D/A (Gy/GBq)	D (Gy)	D/A (Gy/GBq)	D (Gy)
Pat 1 - Les 1	Latero-cervical lymph-nodes	83.9	3.2	33.9	0.9	10.3
Pat 1 - Les 2	Pelvic tissue	21.9	7.2	75.8	4.0	43.1
Pat 3 - Les 1	Left retroclavear lymph-nodes	4.3	26.1	276.7	10.1	128.3
Pat 3 - Les 2	Right retroclavear lymph-nodes	0.4	15.8	167.1	11.1	141.1
Pat 3 - Les 3	Thoracic paravertebral tissue	61.4	5.6	58.8	2.1	26.7
Pat 4 - Les 1	Cervico-mediastinic lymph-nodes	4.8	14.7	129.2	3.4	6.3
Pat 5 - Les 1	Mediastinic lymph-nodes	0.4	25.1	220.9	6.4	70.6
Pat 5 - Les 2	Left retroclavear lymph-nodes	0.9	10.6	93.7	6.7	73.6
Pat 6 - Les 1	Abdominal paravertebral tissue	14.4	18.3	284.8	18.9	300.9
Pat 7 - Les 1	Cervico-mediastinic lymph-nodes	246.4	8.2	143.9	6.4	114.3
Pat 8 - Les 1	Mediastinic lymph-nodes	2.8	6.2	57.3	3.3	36.3
Pat 10 - Les 1	Abdominal mass	31.9	8.9	87.8	10.8	101.6
Pat 11 - Les 1	Latero-cervical lymph-nodes	98.6	21.4	70.8	20.5	70.2

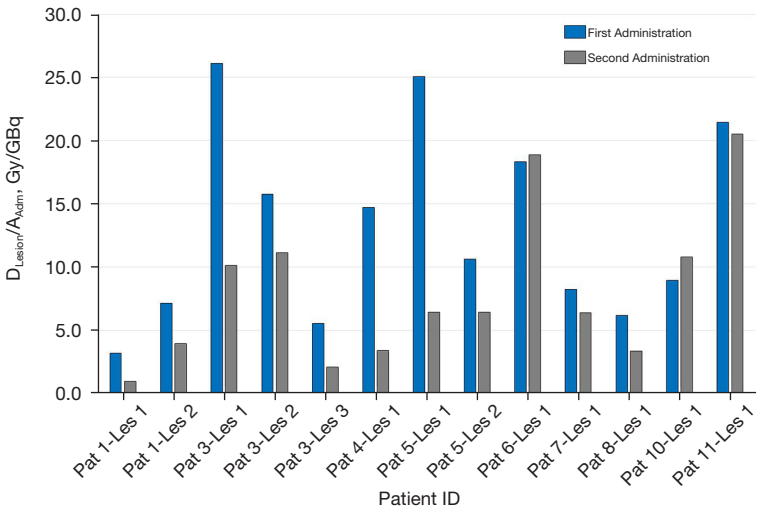

Figure 5 Comparison between D_{Lesion}/A_{Adm} values assessed at first (blue) and at second (gray) administration.

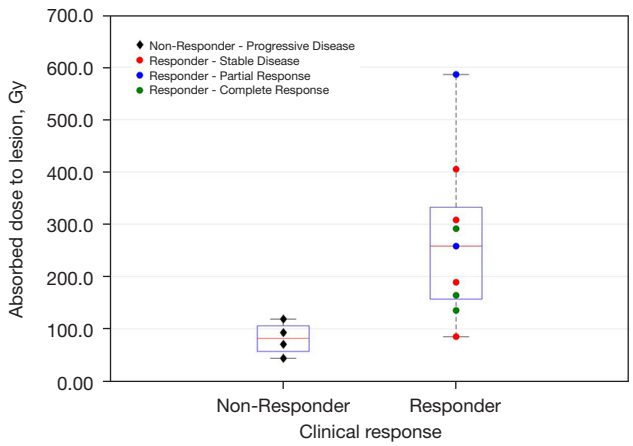

Figure 6 Therapeutic dose-response graph. The total doses to lesions are divided into groups based on the clinical response.

value after the two administrations were close to the dose of 4 Gy in 8 patients (in the range of 3.5–4.5 Gy). Four patients (2,7,9,13) over 50 kg of weight reached an absorbed dose to WB within the range 1.5 to 3.0 Gy since it was not possible to administer a higher activity than 17 GBq due to legal limits. The remaining 2 patients (1 and 8 with a weight of 27 and 21 kg respectively) showed a variability of D_{WB}/A_{Adm} between the first and the second administration (around 25%) reaching an absorbed dose of 2.9 and 3.2 Gy respectively.

In 2015, Mínguez *et al.* (22) studied the correlation between D_{WB}/A_{Adm} and patient's mass, using data of 3 different studies (22,24,25) and obtaining the following relationship:

$$\frac{D_{WB}}{A_{Adm}} = 3.63 \cdot m^{-0.921} \quad [9]$$

From the comparison of the two results (*Figure 4*) it is possible to note that the two curves are very similar, with a percentage difference equal to 4.3%. The correlation is very strong as underlined by the R^2 value of 0.9214. However, the maximum distance between data and fit is around 43%, consequently, equation number 9 can be used in a first approximation for the choice of the activity to be administered but patient's dosimetry is still necessary in order to obtain a reliable dose value.

Generally the calculation of the absorbed dose to RM is not performed for patient affected by rrmHR-NBL treated with two administration of ^{131}I-mIBG. Blood sample collection was not a painful procedure due to the presence of a CLC generally placed for clinical purpose in oncological patient submitted to heavy treatment. For this reason it has been possible to collect 6–7 blood samples from each patient. In the present protocol, the dose limit to WB of the entire treatment is set at 4 Gy without considering quantitative prescriptions on dosimetry to RM. Reviewing the literature about analogous dosimetric protocol, Giammarile *et al.* in EANM guideline procedure sets the dose limit to red marrow at 2 Gy (26) in order to avoid marrow toxicity. Analyzing the D_{RM}, these values were higher than 2 Gy in 50% of patients (maximum value 2.6 Gy).

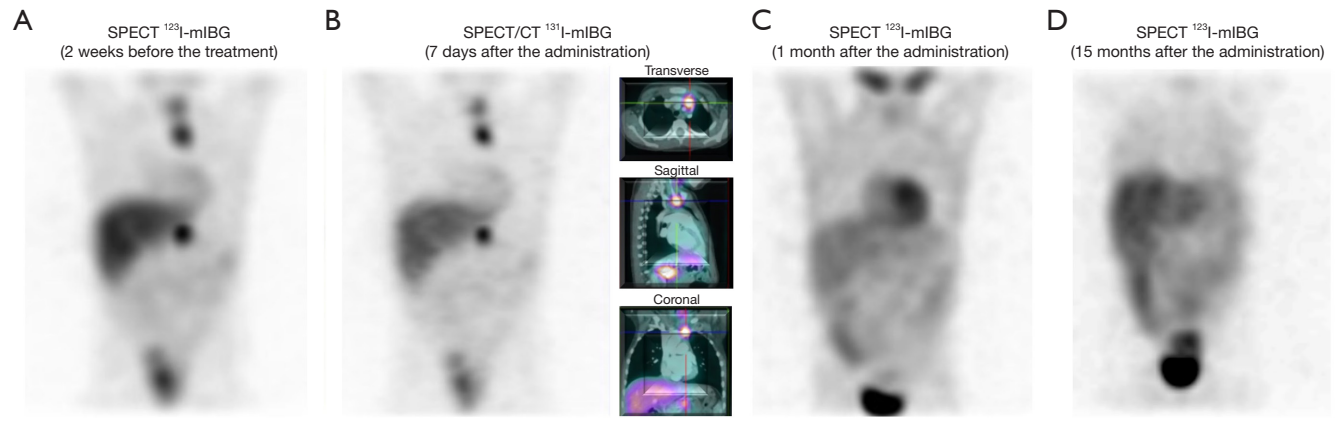

Figure 7 The clinical history of a Complete Response case. A 4-year-old girl with diagnosis of stage IV NBL at 2 years (abdominal mass associated with cervical and thoracic localization and bone involvement) was treated according to SIOPEN NBHR 01 protocol. At the end of induction chemotherapy, a new balance of disease by mIBG scan showed a complete skeletal response with a partial response of soft tissue lesions. Abdominal residual mass was submitted to partial surgical resection and radiotherapy while cervical and thoracic lesions showed a progression of disease. The patient was referred to ^{131}I-mIBG high activity therapy after pre-treatment ^{123}I mIBG evaluation (A) and confirmed by imaging after ^{131}I mIBG therapy (B). The D_{Lesion} was equal to 129.2 Gy. The patient showed an early complete response at 1 month after the ^{131}I-mIBG administration (C) and confirmed at last follow-up (D).

This result is not in contradiction with the literature data because myeloablation is a deterministic effect required in the treatment protocol in preparation for bone marrow transplantation.

Considering the D_{WB}/A_{Adm} values (reported in *Figure 1B* and *Figure 2* for WB and RM, respectively) and calculating the percentage difference between the first and the second administrations it is possible to assume that the first result is predictive of the second one; infact, in the majority of the cases (9/13), the differences is less than 10%.

Figure 3 shows the correlation between D_{WB} and D_{RM} confirming the linear correlation obtained by Mínguez *et al.* with a percentage differences between the angular coefficients equals to 6.25%. The small contribution of self blood to D_{RM} (about 10%), showed in *Figure 2* could explain the strong agreement between D_{WB} and D_{RM} reported in *Figure 3*.

It should be considered that dosimetric implementation in pediatric practice requires particular skills and a dedicated multidisciplinary team (pediatric nuclear medicine staff, oncologists, medical physicists) in order to obtain the best collaboration according to the patient's age. Furthermore, in literature there is a limitated experience in dosimetric approach about radionuclide therapy in a pediatric setting; a dosimetric assessment including D_{RM} and D_{WB} could be helpful to have a complete data panel to define a reliable standardized procedure.

In order to have a deeper understanding regarding lesions uptake and relative metastatic response, we assessed absorbed dose to lesions by planar dosimetric approach, when feasible.

Concerning the lesions dosimetry, the doses distribution shows a wide range of calculated values on the first administration (33.9–284.8 Gy). This variability depends on multiple factors related to lesion volume, uptake and effective half-life. Furthermore, the obtained results are comparable with those reported in literature in similar studies (27).

Analysis of *Figure 5* and *Table 3*, a high number of lesions appears to have an uptake reduction between the first and second administration, due to radiosensitivity phenomenon and to the reduction of the lesion size. Therefore it is possible to state that the first administration may not be predictive for the second which will potentially deliver a lower dose.

Figure 7 summarizes all clinical efforts to overcome the complex aspects linked to this challenge disease reporting a case of complete response. Otherwise, analysing "Non Responder" cases by dosimetric data allows to have a deeper understanding of limitative factors to obtain a therapeutic response.

In *Figure 6*, it is possible to note that there is a

distinction between the two groups of response (Responder and Non-Responder) with a threshold value near to 120 Gy, confirming that the absorbed dose to lesions could be a good indicator for patients outcome as stated in (27). The value of 120 Gy is considerably higher than the 70 Gy administered in a single injection by Mhattay *et al.* Biological Effective Dose (BED) assessment could allow to overcome the limits in comparing studies, but in neuroblastoma disease a broad range of values have been reported in literature for radiobilogical factor (α/β: 1.85–17.59 Gy; μ: 0.46–1.28 h^{-1}) (28) resulting in a high variability BED estimation.

Further investigations and a higher number of cases are needed to understand if the absorbed dose to lesions could give important prognostic information predicting patient's treatment response. The small number of the analyzed sample and the numerical difference of the two groups lead to a large uncertainty in the estimation of the dose threshold.

The main drawbacks of the present study are due to the intrinsic limits of planar method which does not allow dosimetric assessment for overlapped uptake areas. In most of our cases, lesions were placed in retro-hepatic site and the physiological liver uptake limited the applicability of planar dosimetric approach. All this limits could justify the case of a low absorbed dose to lesions with a good clinical response (as reported in *Figure 6*). Despite the aforementioned limits, analizing each single case we observed a good agreement between the D_{Lesion} value (quantitatively calculated) and the clinical response status (assessed by locoregional and global qualitative comparison of pre/post treatment ^{123}I-mIBG scan).

SPECT/CT imaging for tumor dosimetry (3D and voxel dosimetry) overcomes planar limits about critical site and lesion heterogeneity, especially in neuroblastoma disease.

A relatively limited number of whole-body measurements were performed compare to the gold standard protocol [as reported by Gear *et al.* (20)] due to the lack of a ceiling-mounted Geiger counter. However, 6–7 measurements performed by highly reproducible and accurate methods could still guarantee sufficiently reliable results.

Recent trials have focused on integrated treatment strategies in order to improve the poor prognosis in rrmHR-NBL patients. VERITAS trial (29) represents an encouraging therapeutic approach for very high-risk neuroblastoma clinical management applying intensive high-dose ^{131}I-mIBG therapy in case of poor responder patients after induction chemotherapy. The efficacy of this international therapeutic program including the use of metabolic radiotherapy will be assessed compared with a classic treatment with myeloablative chemotherapy. This intensive treatment strategy combines the radiosensitiser effect of topotecan with the maximized therapeutic efficacy of radionuclide, followed by BuMel (busulfan and melphalan) as myeloablative regimen followed by peripheral blood stem cell rescue. The synergic treatments effect has the therapeutic goal to allow keeping a high anti-proliferative activity against disease. Furthermore, multicentric approach of VERITAS trial allows to obtain stronger results overcoming the limited number of patients with this rare disease submitted to high doses of ^{131}I-mIBG therapy. Tailored treatment approaches based on dosimetry allows to include radionuclide therapy into systemic chemotherapy and myeloablative transplantation protocols maximizing the treatment benefits ensuring a high safety profile. Our experience enforces the confidence the personalized dosimetry could give a significant contribution in patient care affected by high-risk neuroblastoma. We applied high activity therapy ^{131}I-mIBG protocol (as two administration intensive strategy) in heavily pre-treated rrmHR-NBL children; as soon as approved in Italy, we will take part to VERITAS protocol using radionuclide therapy to improve the understanding of its efficacy in poor responder children affected by very high-risk disease. The future implementation of 3D and voxel dosimetry on SPECT/CT imaging will overcome limits of planar dosimetric approach allowing a more accurate assessment of absorbed dose to lesions, regardless of tumor site.

Acknowledgments

We thank Dr. Maria Concetta Longo for taking part at the early phase of our experience presenting our preliminary data at EANM 18 congress; we thank Dr. Elisabetta Genovese for the support; we thank Dr Federica Martire and Davide Ciucci for helping us to calculate the absorbed dose.

Funding: None.

Footnote

Reporting Checklist: The authors have completed the STROBE reporting checklist. Available at https://dx.doi.org/10.21037/qims-21-548

Conflicts of Interest: All authors have completed the ICMJE

uniform disclosure form (available at https://dx.doi.org/10.21037/qims-21-548). The authors have no conflicts of interest to declare

Ethics Statement: The authors are accountable for all aspects of the work in ensuring that questions related to the accuracy or integrity of any part of the work are appropriately investigated and resolved. The study was conducted in accordance with the Declaration of Helsinki (as revised in 2013). The study was approved by ethics committee of IRCCS Bambino Gesù Children's Hospital and informed consent was taken from all individual participants.

References

1. Zage PE. Novel Therapies for Relapsed and Refractory Neuroblastoma. Children (Basel) 2018;5:148.
2. London WB, Castel V, Monclair T, Ambros PF, Pearson AD, Cohn SL, Berthold F, Nakagawara A, Ladenstein RL, Iehara T, Matthay KK. Clinical and biologic features predictive of survival after relapse of neuroblastoma: a report from the International Neuroblastoma Risk Group project. J Clin Oncol 2011;29:3286-92.
3. Matthay KK, Yanik G, Messina J, Quach A, Huberty J, Cheng SC, Veatch J, Goldsby R, Brophy P, Kersun LS, Hawkins RA, Maris JM. Phase II study on the effect of disease sites, age, and prior therapy on response to iodine-131-metaiodobenzylguanidine therapy in refractory neuroblastoma. J Clin Oncol 2007;25:1054-60.
4. Wilson JS, Gains JE, Moroz V, Wheatley K, Gaze MN. A systematic review of 131I-meta iodobenzylguanidine molecular radiotherapy for neuroblastoma. Eur J Cancer 2014;50:801-15.
5. Matthay KK, Tan JC, Villablanca JG, Yanik GA, Veatch J, Franc B, Twomey E, Horn B, Reynolds CP, Groshen S, Seeger RC, Maris JM. Phase I dose escalation of iodine-131-metaiodobenzylguanidine with myeloablative chemotherapy and autologous stem-cell transplantation in refractory neuroblastoma: a new approaches to Neuroblastoma Therapy Consortium Study. J Clin Oncol 2006;24:500-6.
6. French S, DuBois SG, Horn B, Granger M, Hawkins R, Pass A, Plummer E, Matthay K. 131I-MIBG followed by consolidation with busulfan, melphalan and autologous stem cell transplantation for refractory neuroblastoma. Pediatr Blood Cancer 2013;60:879-84.
7. Gaze MN, Chang YC, Flux GD, Mairs RJ, Saran FH, Meller ST. Feasibility of dosimetry-based high-dose 131I-meta-iodobenzylguanidine with topotecan as a radiosensitizer in children with metastatic neuroblastoma. Cancer Biother Radiopharm 2005;20:195-9.
8. Lewington V, Lambert B, Poetschger U, Sever ZB, Giammarile F, McEwan AJB, Castellani R, Lynch T, Shulkin B, Drobics M, Staudenherz A, Ladenstein R. 123I-mIBG scintigraphy in neuroblastoma: development of a SIOPEN semi-quantitative reporting ,method by an international panel. Eur J Nucl Med Mol Imaging 2017;44:234-41.
9. Park JR, Bagatell R, Cohn SL, Pearson AD, Villablanca JG, Berthold F, Burchill S, Boubaker A, McHugh K, Nuchtern JG, London WB, Seibel NL, Lindwasser OW, Maris JM, Brock P, Schleiermacher G, Ladenstein R, Matthay KK, Valteau-Couanet D. Revisions to the International Neuroblastoma Response Criteria: A Consensus Statement From the National Cancer Institute Clinical Trials Planning Meeting. J Clin Oncol 2017;35:2580-7.
10. Kletting P, Schimmel S, Kestler HA, Hänscheid H, Luster M, Fernández M, Bröer JH, Nosske D, Lassmann M, Glatting G. Molecular radiotherapy: the NUKFIT software for calculating the time-integrated activity coefficient. Med Phys 2013;40:102504.
11. Glatting G, Kletting P, Reske SN, Hohl K, Ring C. Choosing the optimal fit function: comparison of the Akaike information criterion and the F-test. Med Phys 2007;34:4285-92.
12. Hindorf C, Glatting G, Chiesa C, Lindén O, Flux G; EANM Dosimetry Committee. EANM Dosimetry Committee guidelines for bone marrow and whole-body dosimetry. Eur J Nucl Med Mol Imaging 2010;37:1238-50.
13. Buckley SE, Saran FH, Gaze MN, Chittenden S, Partridge M, Lancaster D, Pearson A, Flux GD. Dosimetry for fractionated (131)I-mIBG therapies in patients with primary resistant high-risk neuroblastoma: preliminary results. Cancer Biother Radiopharm 2007;22:105-12.
14. Stabin MG, Siegel JA. Physical models and dose

factors for use in internal dose assessment. Health Phys 2003;85:294-310.
15. Giostra A, Richetta E, Pasquino M, Miranti A, Cutaia C, Brusasco G, Pellerito RE, Stasi M. Red marrow and blood dosimetry in (131)I treatment of metastatic thyroid carcinoma: pre-treatment versus in-therapy results. Phys Med Biol 2016;61:4316-26.
16. Stabin MG, Siegel JA, Sparks RB. Sensitivity of model-based calculations of red marrow dosimetry to changes in patient-specific parameters. Cancer Biother Radiopharm 2002;17:535-43.
17. Stabin MG, Sparks RB, Crowe E. OLINDA/EXM: the second-generation personal computer software for internal dose assessment in nuclear medicine. J Nucl Med 2005;46:1023-7.
18. Siegel JA, Thomas SR, Stubbs JB, Stabin MG, Hays MT, Koral KF, Robertson JS, Howell RW, Wessels BW, Fisher DR, Weber DA, Brill AB. MIRD pamphlet no. 16: Techniques for quantitative radiopharmaceutical biodistribution data acquisition and analysis for use in human radiation dose estimates. J Nucl Med 1999;40:37S-61S.
19. Ogawa K, Harata Y, Ichihara T, Kubo A, Hashimoto S. A practical method for position-dependent Compton-scatter correction in single photon emission CT. IEEE Trans Med Imaging 1991;10:408-12.
20. Gear J, Chiesa C, Lassmann M, Gabiña PM, Tran-Gia J, Stokke C, Flux G; EANM Dosimetry Committee. EANM Dosimetry Committee series on standard operational procedures for internal dosimetry for 131I mIBG treatment of neuroendocrine tumours. EJNMMI Phys 2020;7:15.
21. Sgouros G. Blood and bone marrow dosimetry in radioiodine therapy of thyroid cancer. J Nucl Med 2005;46:899-900; author reply 901.
22. Mínguez P, Flux G, Genollá J, Guayambuco S, Delgado A, Fombellida JC, Sjögreen Gleisner K. Dosimetric results in treatments of neuroblastoma and neuroendocrine tumors with (131)I-metaiodobenzylguanidine with implications for the activity to administer. Med Phys 2015;42:3969-78.
23. Genolla J, Rodriguez T, Minguez P, Lopez-Almaraz R, Llorens V, Echebarria A. Dosimetry-based high-activity therapy with 131I-metaiodobenzylguanidine (131I-mIBG) and topotecan for the treatment of high-risk refractory neuroblastoma. Eur J Nucl Med Mol Imaging 2019;46:1567-75.
24. Toporski J, Garkavij M, Tennvall J, Ora I, Gleisner KS, Dykes JH, Lenhoff S, Juliusson G, Scheding S, Turkiewicz D, Békássy AN. High-dose iodine-131-metaiodobenzylguanidine with haploidentical stem cell transplantation and posttransplant immunotherapy in children with relapsed/refractory neuroblastoma. Biol Blood Marrow Transplant 2009;15:1077-85.
25. Buckley SE, Chittenden SJ, Saran FH, Meller ST, Flux GD. Whole-body dosimetry for individualized treatment planning of 131I-MIBG radionuclide therapy for neuroblastoma. J Nucl Med 2009;50:1518-24.
26. Giammarile F, Chiti A, Lassmann M, Brans B, Flux G; EANM. EANM procedure guidelines for 131I-meta-iodobenzylguanidine (131I-mIBG) therapy. Eur J Nucl Med Mol Imaging 2008;35:1039-47.
27. Matthay KK, Panina C, Huberty J, Price D, Glidden DV, Tang HR, Hawkins RA, Veatch J, Hasegawa B. Correlation of tumor and whole-body dosimetry with tumor response and toxicity in refractory neuroblastoma treated with (131) I-MIBG. J Nucl Med 2001;42:1713-21.
28. Mínguez P, Gustafsson J, Flux G, Gleisner KS. Biologically effective dose in fractionated molecular radiotherapy--application to treatment of neuroblastoma with (131) I-mIBG. Phys Med Biol 2016;61:2532-51.
29. Trial Evaluating and Comparing Two Intensification Treatment Strategies for Metastatic Neuroblastoma Patients With a Poor Response to Induction Chemotherapy (VERITAS). Available online: https://clinicaltrials.gov/ct2/show/NCT03165292

Cite this article as: Cassano B, Pizzoferro M, Valeri S, Polito C, Donatiello S, Altini C, Villani MF, Serra A, Castellano A, Garganese MC, Cannatà V. Personalized dosimetry for a deeper understanding of metastatic response to high activity ^{131}I-mIBG therapy in high risk relapsed refractory neuroblastoma. Quant Imaging Med Surg 2022;12(2):1299-1310. doi: 10.21037/qims-21-548

